Lanthanum samarium oxalate — Its growth and structural characterization

VARUGHESE JOHN, M A ITTYACHEN and K S RAJU*

School of Pure and Applied Physics, Mahatma Gandhi University, Kottayam 686 031, India
*Department of Crystallography and Biophysics, University of Madras, Guindy Campus, Madras 600 025, India

Abstract. Lanthanum samarium oxalate (LSO) single crystals are grown in silica gels by the diffusion of a mixture of aqueous solutions of lanthanum nitrate and samarium nitrate into the test tube having the set gel impregnated with oxalic acid. Tabular crystals of LSO having well defined hexagonal basal planes are observed at different depths inside the gel. LSO crystals grown by this method are colourless and transparent. Laue transmission X-ray diffraction pattern of LSO reveals well defined spots with two-fold symmetry along the horizontal axis. Thermogravimetric analysis (TGA) and differential scanning calorimetry (DSC) support that LSO loses water around 120°C, and CO and CO_2 around 350–450°C. The infrared (IR) absorption spectrum of LSO establishes the presence of oxalate $(C_2O_4)^{2-}$ ions. Energy dispersive X-ray analysis (EDAX) confirms the presence of La and Sm in the sample. X-ray photoelectron spectroscopic (XPS) studies of LSO confirm the presence of La and Sm in their respective oxide states. An empirical structure for LSO has been proposed on the basis of these findings.

Keywords. Lanthanum samarium oxalate crystals; growth; UV-visible; XRD; TGA; DSC; IR; EDAX; XPS.

1. Introduction

The compounds of rare earth especially oxalates and molybdates have gained importance for their ferroelectric and ferroelastic behaviour, which find applications in electro and acousto optical devices (Barkley *et al* 1971, 1972; Sapriel and Vacher 1977). Rare earth based compounds also exhibit high temperature superconductivity and oxalate crystals show ionic conductivity (George *et al* 1990). Superconducting compounds have been synthesized by the controlled precipitation of oxalates followed by calcination (Caillaud *et al* 1988). Beille *et al* (1987) reported that lanthanum copper oxide exhibits superconductivity up to 40 K. Tetragonal bipyramidal crystals of barium oxalate are grown by the precipitation of alkaline earth metal oxalate powders from the neutral aqueous solutions (Pacter 1977). Employing Czochralski technique, rare earth oxalates (R = La, Sm, Nd, Tb and Dy) are grown at elevated temperatures (Brixner 1973). Thermal stresses introduced during growth make these crystals defective. To avoid these defects, crystal growth methods at room temperatures are preferred. For the growth of inorganic crystals, which are sparingly soluble, it is established that gel technique pioneered by Henisch *et al* (1965) and Henisch (1970), is found to be the most suitable. Despite the limitations in the sizes of the gel grown crystals, this technique has been fully exploited for investigating the growth morphologies (Raju 1983a, b; Jayakumar and Raju 1983), the nature of dislocations (Raju 1985) and the mechanical behaviour (Raju *et al* 1984) in the case of synthetic gypsum. The crystals of rare earth
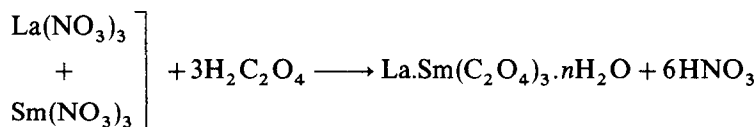
---

*Author for correspondence

mixed oxalates and molybdates grown by gel method at room temperature are characterized employing several techniques (Raju *et al* 1994; Sushma Bhat *et al* 1995; Jayakumari *et al* 1995). The authors report here the work carried out on the growth of LSO in gels, besides their characterization, employing UV-visible, XRD, TGA, IR, EDAX and XPS techniques. These findings throw light in understanding the kinetics of chemical reactions, thermal stability, the detection of heavy elements present in the mixed oxalates, as well as the identification of their chemical states. The empirical structure of LSO sample has been proposed and discussed on the basis of these findings.

2. Experimental and results

2.1   *Growth of LSO in gels*

Sodium meta silicate solution in distilled water (specific gravity: $1\cdot04\,g\,cm^{-3}$) is adjusted to the desired pH by adding analytical grade nitric acid and used as the reacting medium in a test tube (35 mm dia. and 200 mm in length). A mixture of aqueous solutions of lanthanum nitrate and samarium nitrate with nitric acid is used as the outer reactant above the gel at room temperature. The outer reactant diffuses into the set gel impregnated with oxalic acid and the following reaction takes place producing white colloidal precipitate of mixed oxalates of lanthanum and samarium $(La.Sm(C_2O_4)_3)$ and nitric acid.

$$\left.\begin{array}{c} La(NO_3)_3 \\ + \\ Sm(NO_3)_3 \end{array}\right] + 3H_2C_2O_4 \longrightarrow La.Sm(C_2O_4)_3.nH_2O + 6HNO_3$$

The proposed empirical structure of lanthanum samarium oxalate is given in figure 1. The nucleation from the precipitate results in well-defined isolated tabular crystals with the hexagonal basal plane (figure 2) of relatively bigger sizes at greater depths inside the gel (average size after four weeks: $4 \times 3 \times 2\,mm^3$). The optimum
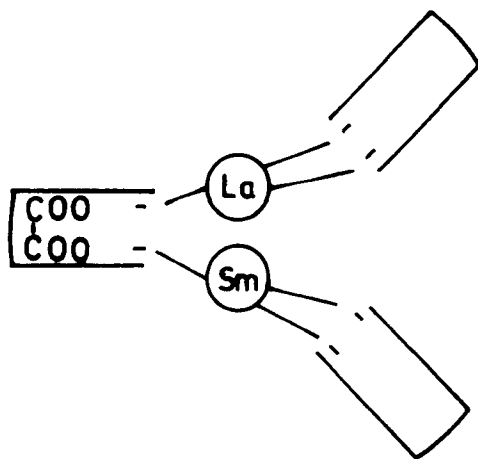

Figure 1.   The proposed empirical structure of LSO.

Figure 2. SEM picture of LSO crystal (× 40).

conditions for the growth of good single crystals of LSO are found to be at pH of 6 of the gel impregnated before setting with 1 M oxalic acid and the mixture of each of the rare earth nitrates in (1:1) by volume as the outer reactant.

2.2 *Characterization of LSO*

2.2a *Experimental*: The UV-visible absorption spectrum of LSO is recorded in Jasco UV-visible spectrometer mode No. (V-530), Japan. The X-ray diffraction patterns of Laue transmission and powdered LSO sample are taken in a Philips XRD PW 1050/70 with CuK_α radiation ($\lambda = 1.5418$ A). The TGA/DSC plots of LSO crystal are recorded using Delta series TGA 7, at the scanning of $20°C/min$. The IR absorption spectrum of LSO sample taken in KBr matrix, is recorded in IR-PERKIN ELMER model 350, England. The sample preparation for EDAX and ESCA is as follows. LSO is finely powdered and pellets of 1 cm dia. and 1 mm thickness are formed using a hydraulic press by applying a pressure of 1.1 tons/cm^2. For EDAX, the surface of LSO pellet mounted onto an aluminium stub is gold coated so as to make a good electrical contact and is examined in the EDAX analyzer No. 711, an accessory to the scanning electron microscope, Philip's SEM model 501. XPS spectra of LSO pellet are recorded in VG scientific ESCALAB MK II, by irradiating the sample with the monochromatic soft X-rays (MgK_α; photon energy 1253.6 eV). The constant analyzer is 50 eV and the resolution of the system is about 0.7 eV.

2.2b *UV-visible spectral studies*: It is interesting to observe in the UV-visible spectrum of LSO that the strong intense peak (in the left hand side of figure 3) around 250 nm is assigned to the oxalate group, as the UV-visible spectrum of oxalic acid solution also reveals this strong peak in position (nm) and intensity. The small peak
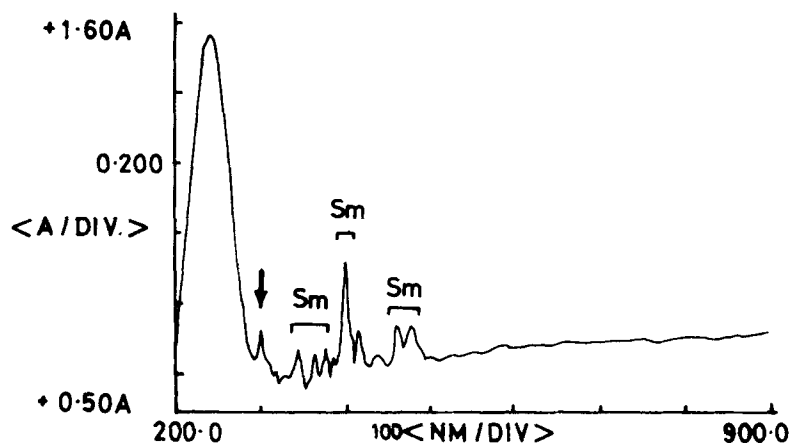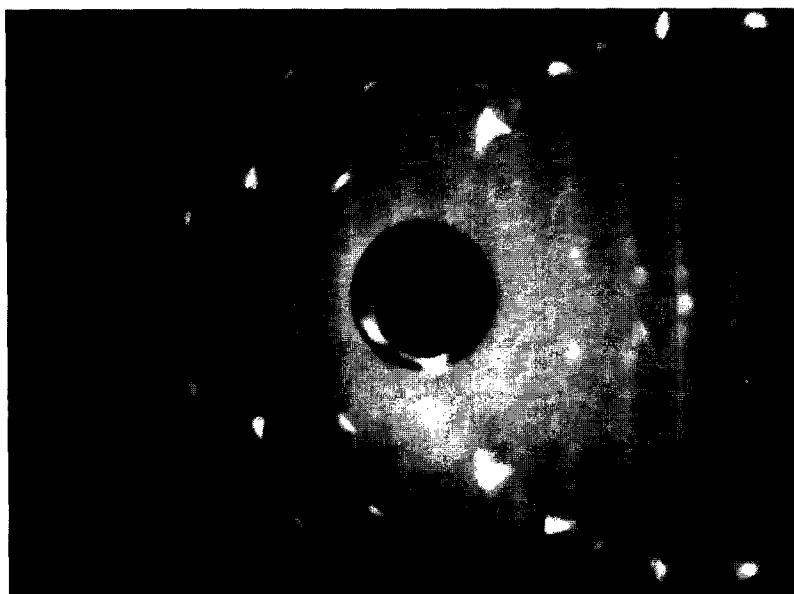
Figure 3. UV-visible spectrum of LSO.

Figure 4. Laue transmission X-ray diffraction pattern of LSO.

(marked by an arrow) next to oxalate peak positioned at 300 nm is attributed to lanthanum in the UV region, as the same is easily detected in the UV-visible spectrum of lanthanum nitrate. The remaining peaks labelled samarium under brackets match exactly with the UV peaks of samarium in the literature (Huheey 1983). It may be mentioned that no peaks are observed in the visible region (from 500–900 nm), indicating that the crystal is transparent for the visible light.

2.2c   *XRD studies*:   The revelation of well defined Bragg peaks at specific (2θ) angles in the XRD of powdered LSO suggests that the sample is ordered. Laue transmission X-ray diffraction of LSO (figure 4) reveals well defined broad and intense Laue spots
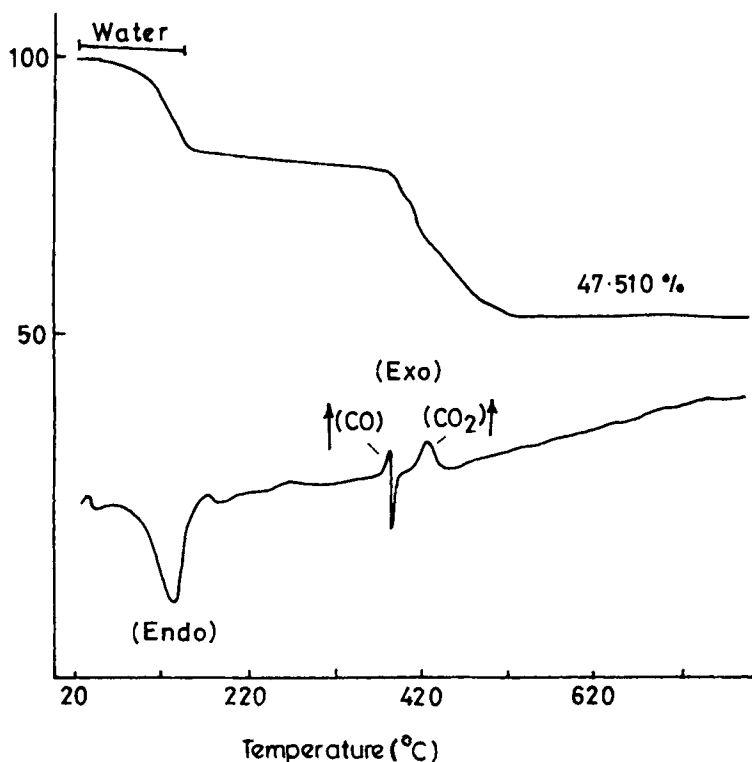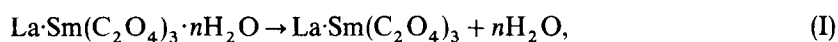
Figure 5. TGA/DSC plots of LSO.

exhibiting two-fold symmetry along the horizontal axis. This strongly gives the clue that LSO is single crystalline in nature. It may be mentioned that even the thin LSO crystal (0·25–0·5 mm) with filtered monochromatic X-rays revealed sharp fine spots of very weak intensity, that too, after 20 h of exposure. Hence, continuous (unfiltered) X-rays was preferred which gave broader Laue spots of high intensity with an exposure of 5 h, as in the present case.

2.2d   *TGA and DSC of LSO*:   The TGA/DSC plots (figure 5) of LSO crystal show the loss of weight in the temperature range around 100°C, relating to the loss of water of crystallization (endothermic reaction) (see equation I below). The loss of weight around 420°C is due to two chemical changes, one relating to release of CO at 400°C and the other at 430°C relating to CO_2, which are exothermic in character and very close to each other (see equation II).

$$La \cdot Sm(C_2O_4)_3 \cdot nH_2O \rightarrow La \cdot Sm(C_2O_4)_3 + nH_2O, \tag{I}$$

$$La \cdot Sm(C_2O_4)_3 \rightarrow La \cdot Sm \ O_3(s) + 3CO(g) + 3CO_2(g). \tag{II}$$

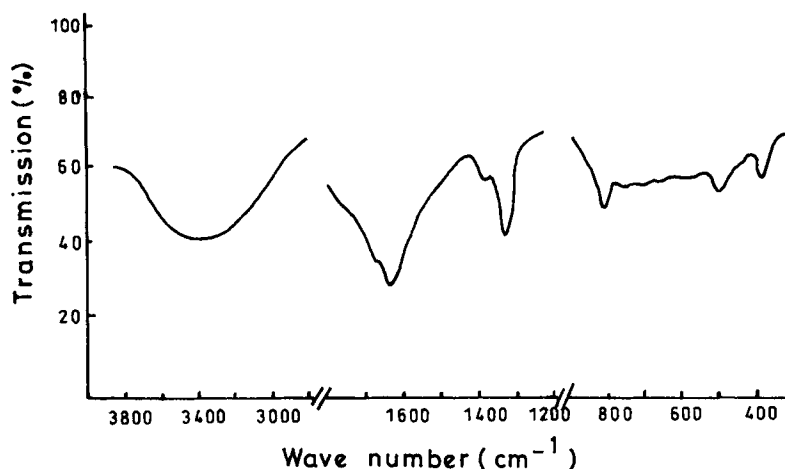$(La \cdot Sm) \ O_3$ is fairly stable and the residue mainly consists of this compound beyond 620°C.

Figure 6. IR absorption spectrum of LSO.

2.2e *IR absorption studies*:   In the IR absorption spectrum of LSO sample (figure 6), the presence of water of crystallization is established by the revelation of well pronounced broad intense peak at $3300 \, cm^{-1}$ relating to asymmetric and symmetric OH stretchings and the peak at $1630 \, cm^{-1}$ relating to HOH bending plus $v_a(C=O)$. The peaks positioned at $1380 \, cm^{-1}$ and the more intense at $1320 \, cm^{-1}$ are attributed to the symmetric stretchings of CO_2. The sharp peak at $810 \, cm^{-1}$ is due to the combined effects of in-plane deformation of CO_2 and the presence of metal-oxygen bonds. The medium peak at $480 \, cm^{-1}$ relates to the rocking of CO_2.

2.2f *EDAX of LSO*:   EDAX work has been taken up to re-establish the elemental incorporation like La and Sm in the LSO sample. The EDAX pattern of LSO is shown in figure 7.

The three peaks positioned at 4·65, 5·04 and 5·38 keV relate to L_α, $L_{\beta 1}$ and $L_{\beta 2}$ energies of lanthanum, while L_α, $L_{\beta 1}$ and $L_{\beta 2}$ energies relating to samarium are represented by peaks positioned at 5·63, 6·2 and 6·58 keV, respectively (figure 7). It may be mentioned that the energy values (keV) reported for La $(L_{\alpha, \beta 1, \beta 2})$ and Sm$(L_{\alpha, \beta 1, \beta 2})$ in the present EDAX investigations are in excellent agreement with the EDAX library.

2.2g *XPS studies*:   XPS studies are undertaken to further establish the constituents incorporated in LSO sample besides their chemical states. XPS peak of C_{1s} of LSO denotes the binding energy of 287 eV, which agrees quite well with the reported value in the literature (Wagner *et al* 1978), and hence the binding energy scale (x-axis) is calibrated. The presence of carbon in the present investigation is attributed to the adventitious hydrocarbon nearly always present from the laboratory environment or from the glove box. Figure 8 shows the XPS peaks relating to La $(3d_{5/2}-3d_{3/2})$ with binding energy centred around 835 eV and 852 eV, with the separation of 16·8 eV, while figure 9 relates to the XPS peak of Sm $(3d_{5/2})$ having the binding energy value at 1083 eV. The XPS region of C_{1s} of LSO sample (figure 10) shows two peaks having binding energies around 287 and 290 eV. The first peak at 287 eV is attributed to the adventitious hydrocarbon, while the second peak at the higher binding energy value of
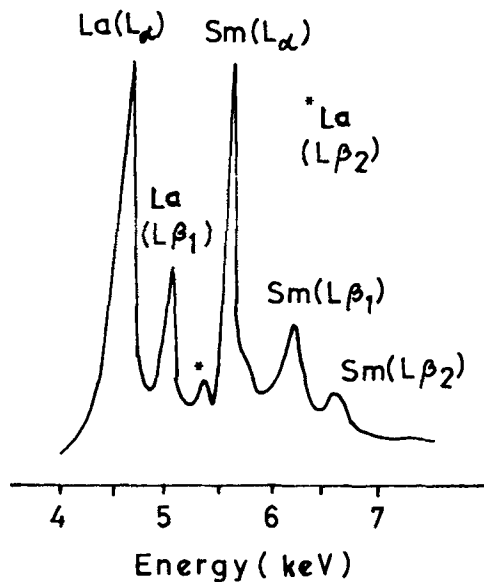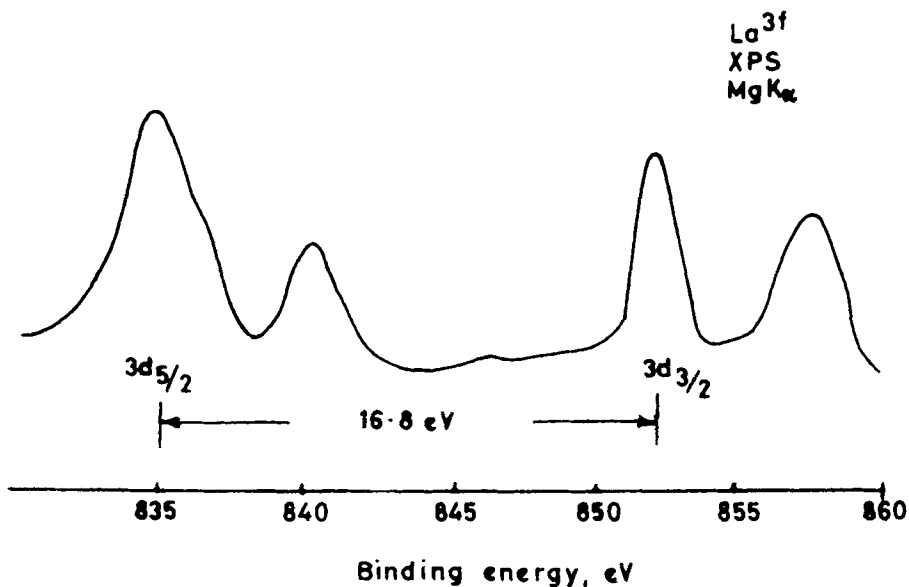
Figure 7. EDAX pattern of LSO.

Figure 8. XPS peaks of La $(3d_{5/2}-3d_{3/2})$ of LSO.

290 eV relates to the oxalate (C_2O_4) group. The second peak relating to the oxalate group is shifted with respect to the first peak towards the higher binding energy value and this is attributed due to higher electronegativity of oxalate group. The binding energy values relating to La $(3d_{5/2}-3d_{3/2})$ and Sm $(3d_{5/2})$ along with separations (figures 8–9) agree quite well with the literature values (Wagner *et al* 1978) corresponding to their oxide states $(La_2O_3$ and $Sm_2O_3)$.
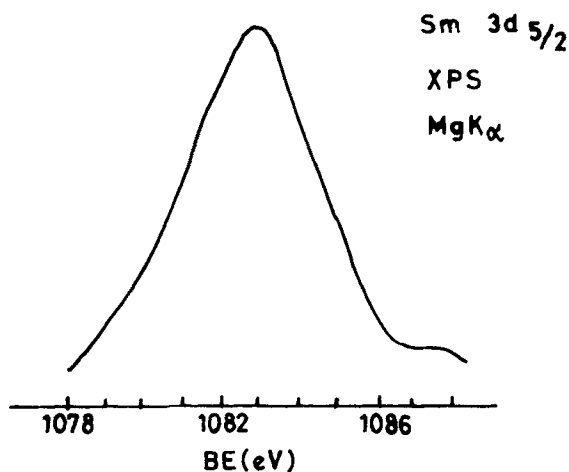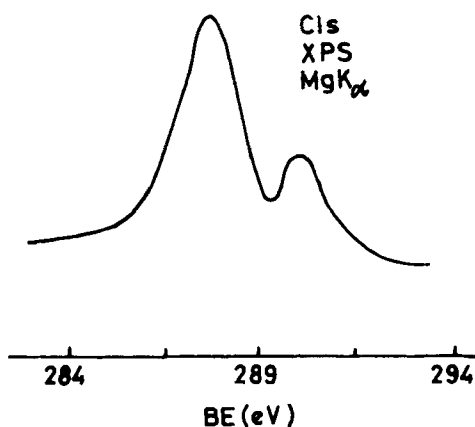
Figure 9.   XPS peak of Sm ($3d_{5/2}$) of LSO.

Figure 10.   XPS peaks of C_{1s} of LSO.

XPS, though a surface analysis, is a well established powerful technique in identifying the constituents present in the sample besides their respective chemical states.

3. Discussion

The gel grown LSO, in the present work, is crystalline in nature which is evident by the revelation of well defined edges and corners with the hexagonal basal planes observed at varying depths in the gel (figure 2). The crystals of LSO are colourless and transparent which is also indicated by the absence of peaks in the visible region in the UV-visible spectrum of LSO (figure 3). The crystalline nature of LSO is evidenced by the revelation of well defined Bragg peaks at specific '2θ' values in the XRD pattern of powdered sample. That LSO is single crystalline, is obviously evidenced by the

revelation of 'Laue spots' with well defined two-fold symmetry (figure 4). TGA/DSC of LSO reveal that the crystals lose water of crystallization around $100-200°C$, and CO and CO_2 around $400-420°C$ and the residue beyond $500°C$ being La and Sm oxides (47.510%) (figure 5). The IR absorption spectrum of LSO (figure 6) establishes the presence of oxalate complex $(C_2O_4)^{2-}$ in the sample. The binding energy values of the EDAX peaks (figure 7) relating to La (L_α, $L_{\beta1,2}$) and Sm (L_α, $L_{\beta1,2}$) agree quite well with the literature values (EDAX library), thereby confirming the incorporation of La and Sm in LSO. The heights and areas (Riggs and Parker 1975) of 'L_α' peaks of La and Sm give the clue that both may have approximately the same affinity to their oxalate formation. The XPS results too, support well that La and Sm are present in the sample besides the existence of these elements in their oxide states (figures 8–9), especially La and Sm getting linked to O^- of $(C_2O_4)^{2-}$. These results are in excellent agreement with the proposed empirical structure for LSO (figure 1).

4. Conclusion

The gel grown LSO sample reported (i) is ordered and crystalline as evidenced by the formation of well defined tabular crystals having hexagonal basal planes, (ii) is colourless and transparent, (iii) is single crystalline in nature (XRD), (iv) accounts for the presence of oxalato complex by the revelation of their characteristic peaks (IR), (v) loses CO and CO_2 around $400°C$ (TGA), (vi) has La and Sm established qualitatively and to some extent quantitatively (EDAX), and (vii) is having La and Sm in their oxide states especially getting linked to O^- of oxalate groups (XPS).

Acknowledgements

References

Barkley J R, Brixner L H and Hogan E M 1971 *IEEE Symposium on the applications of ferroelectrics* (New York: York Town Heights)

Barkley J R, Brixner L H, Hogan E M and Waring R K 1972 *J. Ferroelectrics* **3** 191

Beille J *et al* 1987 *C. R. Acad. Sci. Ser. 2* **304** 1097

Brixner L H 1973 *J. Cryst. Growth* **18** 297

Caillaud F, Baumard J-F and Smith A 1988 *Mater. Res. Bull.* **23** 1273

George V, Ittyachen M A and Jayakumari Isac 1990 *Cryst. Res. Technol.* **25** K-153

Henisch H K 1970 *Crystal growth in gels* (Pennsylvania: Pennsylvania University Press)

Henisch H K, Dennis J and Hanoka J I 1965 *Phys. Chem. Solids* **26** 493

Huheey J E 1983 *Inorganic chemistry – Principles of structure and reactivity* (New York: Harper International) 3rd edition p. 802

Jayakumar D and Raju K S 1983 *Bull. Mater. Sci.* **5** 399

Jayakumari Isac, Ittyachen M A and Raju K S 1995 *Bull. Mater. Sci.* **19** 495

Pacter A 1977 *Krist & Tech.* **12** 729

Raju K S 1983a *J. Mater. Sci. Letts* **2** 705

Raju K S 1983b *Cryst. Res. & Technol.* **18** 1277

Raju K S 1985 *J. Mater. Sci.* **20** 756

Raju K S, Godehardt R, Hopfe J and Pippel E 1984 *Cryst. Res. & Technol.* **19** 1127
Raju K S, Krishna K N, Jayakumari Isac and Ittyachen M A 1994 *Bull. Mater. Sci.* **17** 1447
Riggs W M and Parker M J 1975 *Methods of surface analysis* (ed.) A W Czanderna (Amsterdam: Elsevier Scientific Pub. Co.) Ch. 4, p.108
Sapriel J and Vacher R 1977 *J. Appl. Phys.* **48** 1191
Sushma Bhat, Kotru P N and Raju K S 1995 *Curr. Sci.* **69** 607
Wagner C D, Riggs W M, Davis L E, Moulder J F and Mullenberg J E (eds) 1978 *Handbook of X-ray photoelectron spectroscopy* (Minnesota: Perkin Elmer)